HEFAT2010
7th International Conference on Heat Transfer, Fluid Mechanics and Thermodynamics
19-21 July 2010
Antalya, Turkey

NUMERICAL MODELING AND EXPERIMENTAL INVESTIGATION OF A BIOLOGICALLY-INSPIRED UNDULATING MARINE PROPELLER

González P.B., Rodríguez J.D., Rodríguez C.G., Lamas M.I.*
*Author for correspondence
Departamento de Construcións Navais,
Escola Universitaria Politécnica,
Universidade da Coruña,
Avda. 19 de Febrero s/n, 15405, Ferrol, A Coruña,
Spain,
E-mail: isabellamas@udc.es

ABSTRACT

The study of biologically inspired or fish-like bodies moving in liquid is an interesting and challenging research subject in the field of engineering. An understanding of the complexities of such flows is of interest not only to biologists but also to engineers interested in developing marine vehicles and machines capable of emulating the high performance of fish propulsion.

In the present work, a computational fluid dynamics (CFD) approach using a widely available commercial code was used to investigate the fluid flows around a steady undulating marine propeller when moving in water. This CFD approach yields a complete and complex dataset that allows a detailed investigation of the undulating propulsion. The main objectives of this study were: to quantify the thrust and drag forces acting on the foil, to study the variation of the thrust with the frequency of oscillation and to compare the numerical results with experimental ones.

INTRODUCTION

Throughout history, practical implementation of rotating propulsion mechanisms was highly used because they are very easy to deal with; however, undulating mechanisms, which are very common in the nature, have been poorly considered.

Nowadays, engineering of marine vehicles and machines is maturing and new propulsion methods are being considered. The designs based on biologically-inspired propulsors are being increasingly studied. The problem is that many mechanisms of propulsion are not well understood yet. An important advance which helps to understand the hydrodynamics of biological swimming is the computational fluid dynamics (CFD). There are a lot of researchers who applied the CFD to study biological swimming, for example, Borazjani and Sotiropoulos [1] analyzed numerically the hydrodynamics of the carangiform swimming and then [2] they compared it to the anguilliform swimming for various Reynolds and Strouhal numbers. Carling *et al.* [3] also modelled a self-propelled anguilliform undulatory swimmer using a two-dimensional simplified geometry. Some years later, Kern and Koumoutsakos [4] performed the model with 3D simulations and compared their results with Carling's ones.

Fauci [5] applied the "immersed boundary" method to study neutrally-buoyant organisms and Dillon and Fauci [6] improved this model to include the internal muscle interactions with the external fluid.

Liu *et al.* analized the tadpole propulsion using a two-dimensional numerical model [7] and three-dimensional models [8], [9] and they analized the differences between them.

Tian-jinag *et al.* [10] studied numerically the "*Gymnauchus niloticus*" movement, based on undulations of a long-based dorsal fin aided by two pectoral fins.

Adquins and Yan [11] developed a CFD turbulent model to analyze the motion of a three-dimensional fish tail.

Lewin and Haj-Hariri [12] studied numerically the two-dimensional flow around a sinusoidal airfoil trough a range of frequencies and amplitudes.

Shen *et al.* [13] studied the three-dimensional turbulent flow over a smooth undulating wall undergoing transverse motion in the form of a streamwise travelling wave.

Bozkurtass *et al.* [14] developed a propulsor for an autonomous underwater vehicle based on the mechanical design and performance of the sunfish pectoral fin, based in a three-dimensional numerical model.

For this paper, a two-dimensional model was developed to analize the laminar flow over an undulating propeller. It is organized as follows. Firstly, we will present the details of the model and prescribed kinematics. Secondly, we will briefly

describe the numerical method. Thirdly, we will discuss the hydrodynamic forces and other aspects and compare them with the experimental results. Finally, we will present the conclusions of this work and outline the areas for future research.

NOMENCLATURE

L	[m]	Fin length
t	[s]	Time
F	[N]	Force
A	[m2]	Area
n	[ ]	Unit normal vector
V	[m/s]	Velocity
T	[s]	Period
P	[Pa]	Pressure
g	[m/s^2]	Gravity
Re	[ ]	Reynolds number

Special characters

τ	[N/m^2]	Viscous stress tensor
ρ	[kg/m^3]	Density of the water
ν	[m^2/s]	Kinematic viscosity of the water

Subscripts

x	X direction
p	Pressure
v	Viscosity
max	Maximum

PROBLEM DEFINITION

Design and kinematics

"Innovacións Mariñas" Research Group (Coruña University - Spain) developed an undulanting propeller based on the patent No. 200002012, which author is Primitivo B. Gonzalez [15]. This patent refers to undulating systems and bodies in fluid mediums. The design of the experimental prototype was done from the CFD analysis to assess the most suitable configuration. The experimental prototype, shown in **Figure 1**, consists of an undulating foil propeller of 0.52 m wavelength, 0.02 m amplitude and 0.2 m width.

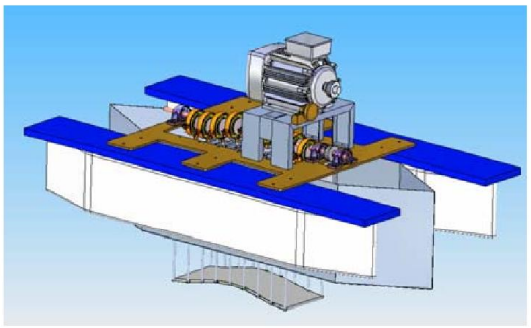

Figure 1. Prototype used for trials.

The main advantage of this system is that it is reversible, *i.e.,* it has the same efficiency either operating forward or backward. This makes it ideal for vehicles that require high maneuverability.

The undulating motion of the fin is created by mean of rods actuating over it, connecting parts and finally the fin. The motion produces a wave shape with constant amplitude along the entire length. The motion is produced by an electric motor and the oscillation frequency of the fin is controlled by a frequency drive control.

Assumptions

In order to simplify the CFD model, the following assumptions were made:

- Laminar flow.
- Incompressible flow.
- Two-dimensional model.
- Gravity is considered.
- Atmospheric pressure.
- Fluid properties of water at 25ºC.

Governing equations

The motion of the flow is governed by the mass conservation equation (1) and momentum conservation equation (2).

$$\nabla \cdot \vec{V} = 0 \tag{1}$$

$$\frac{\delta(\rho \vec{V})}{\delta t} + \nabla \cdot (\rho \vec{V} \vec{V}) = -\nabla p + \nabla \bar{\bar{\tau}} + \rho \vec{g} \tag{2}$$

Equations (1) and (2) were solved numerically to yield the velocity field and the pressure field.

NUMERICAL IMPLEMENTATION

Computational mesh

In order to implement the movement of the fin, a moving mesh was used. The computational domain was 3L height and 5L length (L is length of fin), and was discretized with 27000 nodes. As can be seen in **Figure 2**, the elements were triangular and the size mesh was refined in the zone near the fin.

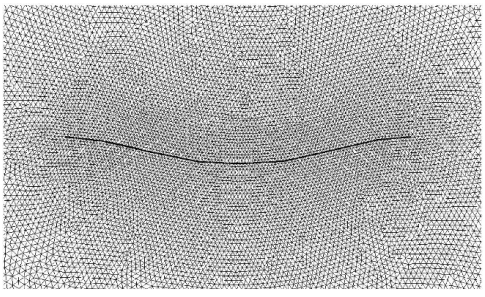

Figure 2. Two-dimensional grid. Only a small part of the overall domain is shown.

Calculation Parameters

The governing equations were solved with the commercial software Ansys Fluent 6.3, which discretizes the equations using the finite volume method (FVM), and the mesh was created with Gambit 2.4

A first-order differencing scheme in time and second-order upwind in space was used and an implicit method was employed for the discretization of the time derivatives.

The period T was divided in 100 parts, *i.e.*, the time step was $\Delta t=T/100$. Both the grid and the time step sensibility of the numerical simulations were studied and it was verified that the size of the computational mesh and time increment employed in the present simulations are adequate to obtain results that are insensitive to further refinement of numerical parameters.

The numerical algorithm implemented in Fluent automatically updates the mesh after each time step relative to the fin's motion using meshing tools such as: "Dynamic layering", to add or remove layers of cells adjacent to a moving boundary based on the height of the layer adjacent to the moving surface; "Spring-based smoothing", to consider the edges between nodes as a network of interconnecting springs and "Local re-meshing" during the spring based smoothing, to minimise convergence problems if a cell becomes too large, too small or excessively stretched and locally re-meshed.

Boundary Conditions

The following boundary conditions were considered:

- Zero velocity at the left wall.
- Slip wall condition at the top and bottom walls.
- Zero gauge pressure at the right wall.
- No slip at the fin.

CALCULATION OF HYDRODYNAMIC FORCES

As the fin moves through the water, a force is produced along the x and y directions. The components of the force acting on the body, F_x and F_y, can be evaluated by integrating the projection of the pressure and the shear stress in the x and y directions respectively. The total thrust component along the x direction was computed by adding the component x of the pressure and viscous forces acting on the body as follows:

$$F_x = F_{px} + F_{vx} \tag{3}$$

where F_p is the pressure force and F_v is the viscous force.

The pressure force along the x axis is given by:

$$F_{px} = -\int_A p n_x dA \tag{4}$$

where n_x is the x component of the unit normal vector on dA.

The viscous force along the x axis is given by:

$$F_{vx} = \int_A \tau_{xj} n_j dA \tag{5}$$

where τ_{xj} is the viscous stress tensor.

RESULTS AND DISCUSSION

In order to reach the steady state with sufficient accuracy, it has been necessary to consider a long time. After several simulations it was verified that, after approximately twenty periods, the time is long enough to reach the steady state. For this reason, all the results given in the present paper correspond to the 20th period of time.

Velocity field

The velocity field for 500 r.p.m. and the 20th period is shown in **Figures 3-6.** This image sequence shows the position of the fin when it gets the maximum and minimum thrust.

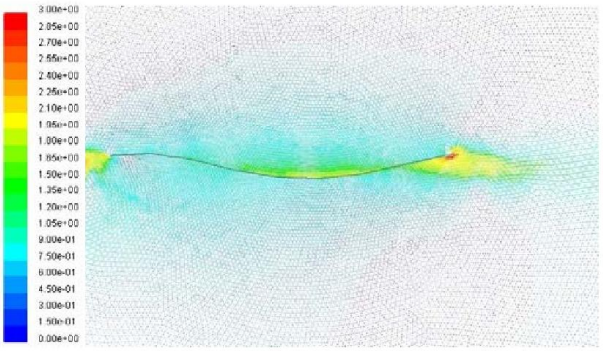

Figure 3. Velocity field for 0.15t/T at 500 r.p.m. (Thrust is minimum).

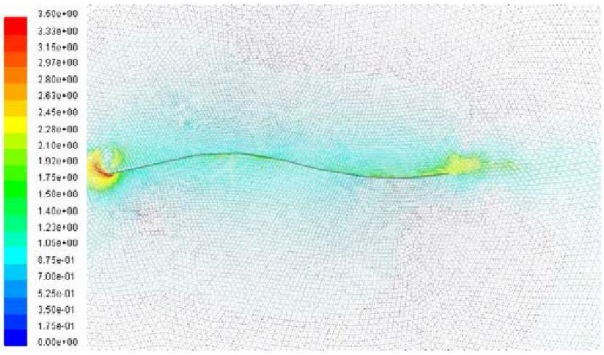

Figure 4. Velocity field for 0.4t/T at 500 r.p.m. (Thrust is maximum).

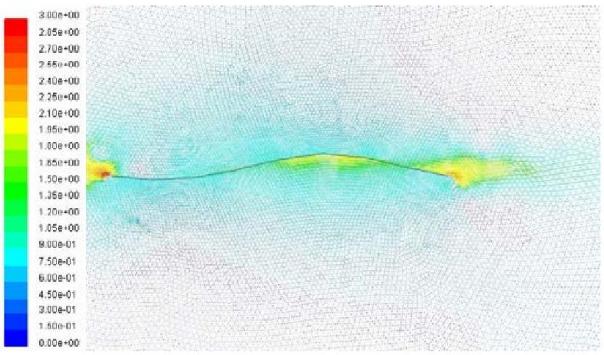

Figure 5. Velocity field for 0.65t/T at 500 r.p.m. (Thrust is minimum).

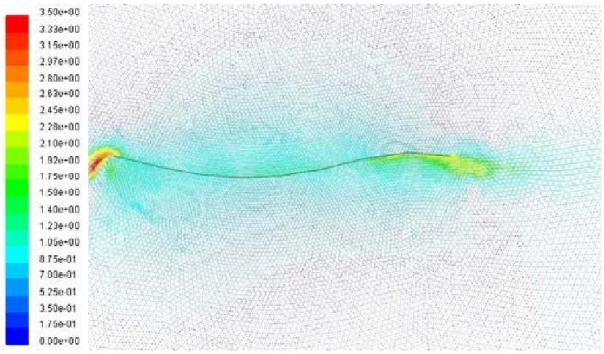

Figure 6. Velocity field for 0.95t/T at 500 r.p.m. (Thrust is maximum).

From **Figures 3-6,** it can be seen that a strong jet is formed at the right side of the fin. This jet is the source of the thrust because it creates a force which tends to move the fin from the right to the left. As the jet separates from the fin, its intensity decreases due to viscous dissipation.

From the figures above, it can also be appreciated that a small jet is formed at the left side of the fin. This jet produces a wasted force which tends to move the fin in the opposite direction. Nevertheless, in all the simulations carried out it was verified that this waste force is much lower than the primary one.

Pressure field

Figure 7 shows the dynamic pressure distribution field for 0.4t/T at 500 r.p.m. It corresponds to **Figure 4**. The effect of the undulating movement on the flow field can be clearly seen and confirms the form of the velocity field. The fluid flow moves from where the pressure is higher to where the pressure is lower, so the tendency of the two jets can be clearly appreciated.

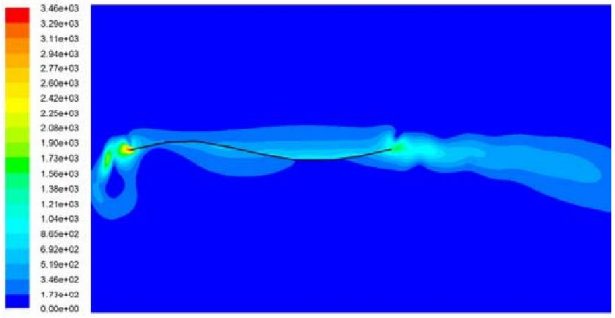

Figure 7. Dynamic pressure field for 0.4t/T at 500 r.p.m.

Hydrodynamic forces

In order to systematically quantify the effect of the fin movement, **Figure 8** was created. This figure represents the time history of the instantaneous pressure force and viscous force. As the viscous force is practically zero, the total force is almost equal to the pressure force. For this reason, only the instantaneous pressure force was represented in **Figure 8**, and the instantaneous total force was omitted.

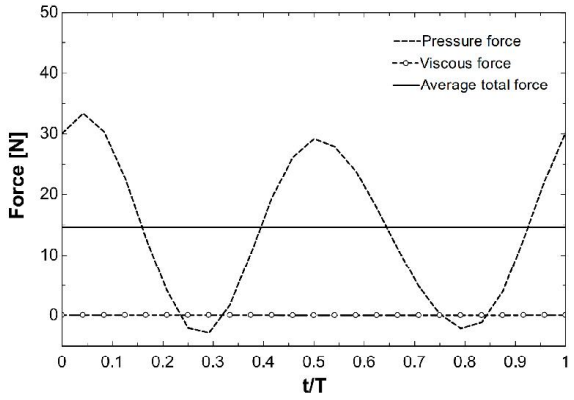

Figure 8. Time history of the pressure force, viscous force and average total force for the 20th period at 500 r.p.m.

It can be observed that the instantaneous pressure force reaches its maximum value twice in each cycle because of the symmetrical undulating movement. The maximum thrust takes place at the time that the ends of the fin are in the position corresponding to a zero amplitude, **Figure 4** and **Figure 6**. The worst case occurs at the point where the edges of the fin are in the position corresponding to its maximum amplitude, **Figure 3** and **Figure 5**.

The viscous force is represented in **Figure 9** with other scale.

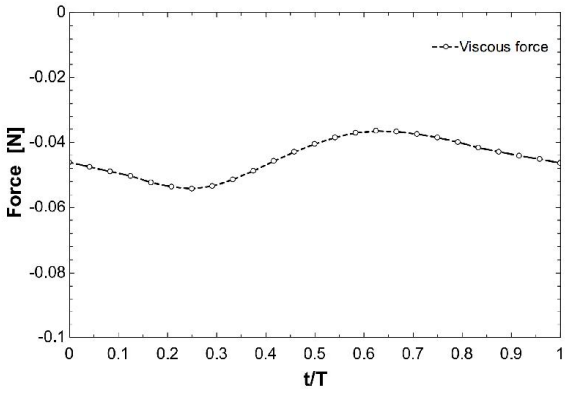

Figure 9. Time history of viscous force for the 20th period at 500 r.p.m.

The forces shown in **Figure 9** are the ones that accelerate the fin either forward or backward, depending on its sign.

In the experimental work it was observed that, apart from the axial force, a small transversal force is produced. This force is zero for the numerical model because it is two-dimensional.

The influence of the frequency was also studied. As expected, the thrust increases when the frequency increases. This is shown in **Figure 10**, which shows the instantaneous total force for 600 r.p.m. and 720 r.p.m.

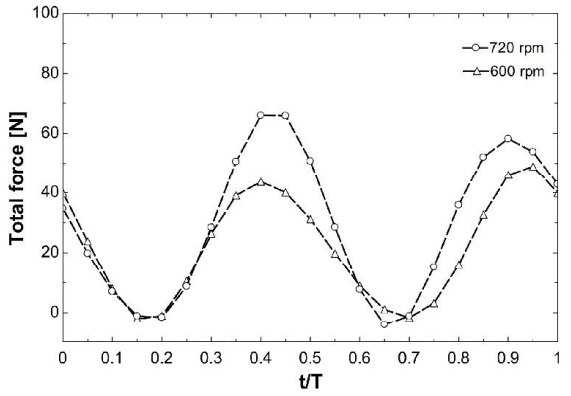

Figure 10. Time history of the total force for the 20th period at 600 r.p.m. and 720 r.p.m.

In order to study this phenomenon in detail, the frequency was incremented from 400 to 1000 r.p.m. and numerical and experimental results were compared. Experimental results were based on the "fixed pull point" method, which consists on fixing the prototype to a bollard by means of a rope, **Figure 11.** Once the prototype was fixed, the force was measured at different frequencies of the electrical motor. A load cell was used to measure these forces and a variable-frequency drive control was used to control the oscillation frequency of the fin.

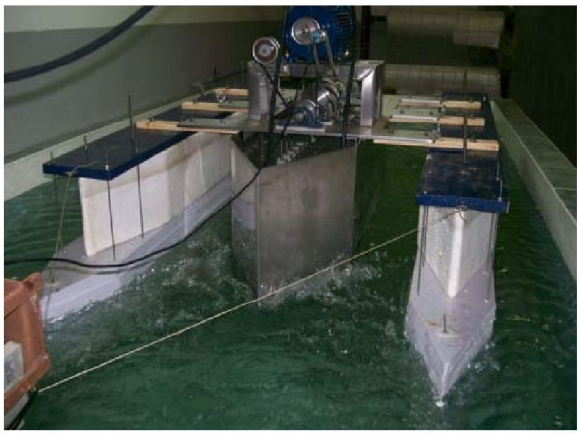

Figure 11. Bollard pull trial under real conditions (fixed pull point).

Numerical and experimental results for the average thrust force against the frequency are compared in **Figure 12.**

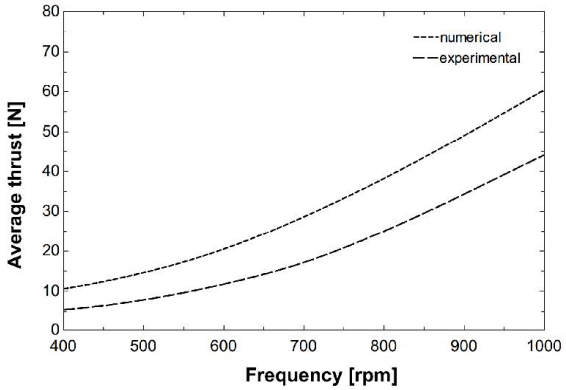

Figure 12. Average force against frequency for numerical and experimental results.

From **Figure 12**, it can be seen that the thrust varies with the frequency following an exponential function. Predicted numerical results are higher than experimental ones because first do not consider three-dimensional losses. For the experimental prototype, it was seen that, apart from the axial force, a transversal force was produced. This force causes wasted power and which can not be computed by a two-dimensional numerical simulation.

Reynolds number

In order to verify that the flow is laminar for the cases studied, the maximum Reynolds number, defined by equation (6), was analized.

$$\mathrm{Re}_{max} = \frac{V_{max} L}{\nu} \qquad (6)$$

Results of the maximum Reynolds number are shown in **Figure 13**. From this figure, it can be seen that the maximum Reynolds number does not exceed the corresponding one to transient laminar-turbulent flow, *i.e.* $5x10^5$, so the assumption of consider laminar flow was correct.

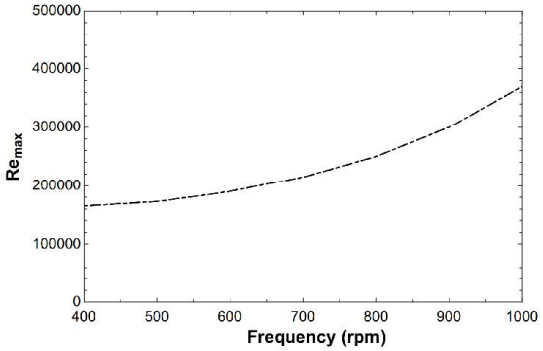

Figure 13. Maximum Reynolds number against frequency.

CONCLUSIONS

This paper proposed a CFD approach to validate an undulating marine propeller. Pressure, viscous and total drag forces were calculated. The results show the maximum thrust produced takes place at the time that the ends of the fin are in the position corresponding to a zero amplitude; the worst case occurs at the point where the edges of the fin are in the position corresponding to its maximum amplitude.

The influence of the frequency was studied and it was found that the net average force is highly dependent on the oscillation frequency of the fin.

A more thorough study on fish locomotion should be done in order to investigate the effect of a three-dimensional model. Until such work is completed, it is difficult to judge whether the effect of removing the two-dimensional restriction will substantially alter the results, particularly the magnitude of the forces acting on the device. Nevertheless, whatever results obtained from the three-dimensional model, the present study is an important step.

Future works including turbulence modeling shall also be needed because it was found that for high frequencies the flow becomes turbulent.

REFERENCES

[1] Borazjani, I. and Sotiropoulos, F., 2008, Numerical investigation of the hydrodynamics of carnguiform in the transitional and inertial flow regimes, *The Journal of Experimental Biology,* vol. 211, pp 1541-1558.

[2] Borazjani, I. and Sotiropoulos, F., 2009, Numerical investigation of the hydrodynamics of an anguilliform swimming in the transitional and inertial flow regimes, *The Journal of Experimental Biology*, vol. 212, pp 577-592.

[3] Carling, J., Williams, T.L. and Bowtell, G., 1998, Self-propelled anguilliform swimming: Simultaneous solution of the two-dimensional Navier-Stokes equations and Newton's laws of motion, *Journal of Experimental Biology*, vol. 201, pp. 3143-3166.

[4] Kern, S., Koumoutsakos, P., 2006, Simulations of optimized anguilliform swimming, *The Journal of Experimental Biology,* 209, pp. 4841-4857.

[5] Fauci, L.J., 1996, A computational model of the fluid dynamics of undulatory and flagellar swimming, *American Zoologist*, vol. 36, pp. 599 607.

[6] Dillon, R.H. and Fauci, L.J., 2000, An integrative model of internal axoneme mechanics and external fluid dynamics in ciliary beating, *Journal of Theoretical Biology*, vol. 207, pp. 415-430.

[7] Liu, H., Wassersug, R.J., and Kawachi, K., 1996, A computational fluid dynamics study of tadpole swimming, *Journal of Experimental Biology*, vol. 199, pp. 1245-1260.

[8] Liu, H., Wassersug, R. and Kawachi, K.,. 1997, The three dimensional hydrodynamics of tadpole locomotion, *Journal of Experimental Biology*, vol. 200, pp. 2807-2819.

[9] Liu, H. and Kawachi, K., 1999, A numerical study of undulatory swimming, *Journal of Computational Physics*, vol. 155, pp. 223-247.

[10] Tian-jinag, H., Lin-cheng, S. and Pei-ling, G., 2006, CFD validation of the optimal arrangement of the propulsive dorsal fin of gymnarchus niloticus, *Journal of Bionic Engineering*, vol. 3, pp. 139-146.

[11] Adkins, D., Yan, Y.Y., CFD simulation of fish-like body moving in viscous liquid, 2006, *Journal of Bionic Engineering*, vol. 3, number 3, pp. 147-153.

[12] Lewin, G.C. and Haj-Hariri, H., 2003, Modelling thrust generation of a two-dimensional heaving airfoil in a viscous flow, *Journal of Fluid Mechanics*, vol. 492, pp. 339-362.

[13] Shen, L., Zhang, X., Yue, D.K.P. and Triantafyllou, M.S., 2003, Turbulent flow over a flexible wall undergoing a streamwise travelling wave motion, *Journal of Fluid Mechanics*, vol. 484, pp. 197-221.

[14] Bozkurttas, M., Tangorra, J., Lauder, G., Mittal, R., 2008,Undersanding the hydrodynamics of swimming: from fish fins to flexible propulsors for autonomous underwater vehicles, *Advances in Science and Technology*, vol. 58, pp. 193-202.

[15] González P.B., Undulating Propulsion System, patent ref. P200002012 (08/10/2003) E.

[16] Fluent 6.3 Documentation, 2006, Fluent Inc.

[17] Gambit 2.4 Documentation, 2007, Fluent Inc.